Chemical Science

ROYAL SOCIETY OF CHEMISTRY

REVIEW

View Article Online
View Journal | View Issue

Cite this: *Chem. Sci.*, 2021, **12**, 12529

Recent advances in heterogeneous catalysis for the nonoxidative conversion of methane

Tianyu Zhang *

The direct conversion of methane to high-value chemicals is an attractive process that efficiently uses abundant natural/shale gas to provide an energy supply. The direct conversion of methane to high-value chemicals is an attractive process that efficiently uses abundant natural/shale gas to provide an energy supply. Among all the routes used for methane transformation, nonoxidative conversion of methane is noteworthy owing to its highly economic selectivity to bulk chemicals such as aromatics and olefins. Innovations in catalysts for selective C–H activation and controllable C–C coupling thus play a key role in this process and have been intensively investigated in recent years. In this review, we briefly summarize the recent advances in conventional metal/zeolite catalysts in the nonoxidative coupling of methane to aromatics, as well as the newly emerging single-atom based catalysts for the conversion of methane to olefins. The emphasis is primarily the experimental findings and the theoretical understanding of the active sites and reaction mechanisms. We also present our perspectives on the design of catalysts for C–H activation and C–C coupling of methane, to shed some light on improving the potential industrial applications of the nonoxidative conversion of methane into chemicals.

Received 14th April 2021
Accepted 26th August 2021

DOI: 10.1039/d1sc02105b

rsc.li/chemical-science

1. Introduction

The conversion of the abundant amount of available methane into high-value chemicals is becoming more attractive owing to the growing depletion of petroleum reserves and proliferation of the availability of natural and shale gas.[1–3] Currently, the indirect route is the most widely used process to produce valuable chemicals from methane.[4] In this method the methane is first converted into syngas (CO and H_2) either by partial oxidation or reforming, and then the products of the long-chain hydrocarbons or alcohols are made from the syngas using Fischer–Tropsch (FT) synthesis.[5] This process causes an additional energy loss and aggravates concerns regarding greenhouse gases, therefore, the direct conversion of methane to high-value chemicals has been considered as an important goal to reduce costs and energy consumption.[6] However, the selective activation of C–H bonds, which has been regarded as a "Holy Grail" in the chemical community, still faces significant challenges owing to the completely symmetrical tetrahedral structure of methane with extremely stable C–H bonds.

To date, many routes, including the oxidative coupling of methane (OCM), partial oxidation of methane (POM), and the nonoxidative coupling of methane (NOCM), have been proposed for the direct conversion of methane into the desired chemical products.[7–9] Although the oxidative methane conversion is thermodynamically feasible, methyl radicals are present in low concentrations and react more easily in the presence of a much higher concentration of oxygen to form $CH_3O_2\cdot$, which is a precursor for the deeper oxidation of methane. Therefore, C_2 hydrocarbons and C_3 in trace amounts are the main products in the OCM depending on the reaction conditions, which reduces the selectivity to desired chemicals and makes the processes uneconomical. In contrast, the nonoxidative conversion of methane is noteworthy owing to its high selectivity to target products such as olefins and aromatics.[10] Nevertheless, a very high reaction temperature is generally required for NOCM as a result of the tremendous thermodynamic barrier, which causes severe coking deactivation of the catalyst.[11] Therefore, significant efforts have been devoted to exploring efficient catalytic systems to enable activation of the methane C–H bond and C–C coupling to improve the NOCM reaction for the efficient utilization of methane.[7,12–14]

Among the catalysts for NOCM, the metal/zeolite based catalysts, such as molybdenum exchanged zeolites, have been extensively studied and show great potential for the aromatization of methane to aromatics.[8] Many properties of the catalyst, including the kind of active metal species, the physical/chemical properties of the supports, as well as the interaction between the metal species and supports, have been proven to be crucial in determining the catalytic performance for the NOCM to aromatics. More recently, the silica matrix-confined single-Fe-atom catalyst (Fe@SiO_2) was reported to realize direct methane conversion to olefins, which is also viewed as a landmark discovery for the transformation of methane.[15] The results of these findings highlight the importance of engineering active

Department of Chemistry, Joint Institute for Advanced Materials, University of Tennessee, Knoxville, TN 37996, USA. E-mail: tzhang29@utk.edu

sites on supports for modulating the selectivity in C–C coupling products. In this review, we summarize the recent experimental advances and theoretical understanding of the conventional metal/zeolite (primarily Mo/zeolite based catalysts) and the newly emerged single-atom catalysts, focusing on the active species, reaction mechanism, and catalytic deactivation for NOCM. Combined with recent progress, prospects for future research on the nonoxidative conversion of methane are also presented.

2. Metal/zeolite catalysts for NOCM

2.1 Mo/zeolite-based catalysts

Since the first report of Mo/HZSM-5 as an efficient catalyst for methane dehydroaromatization (MDA) in 1993,[16] extensive efforts have been devoted to improving the Mo-based catalysts to promote the overall catalytic performances for the NOCM to aromatics by modulating the nature of the metal species, changing the type of zeolite supports, as well as introducing different promoters into the catalysts.

2.1.1 Influence of the nature of the metal species. The nature of the metal species, including the coordination environment, oxidation state, and even the metal loading density, which depends on the preparation methods, significantly influences the target product selectivity and catalytic stability of the methane aromatization reaction.[4,7] For Mo/zeolite catalysts, the location of the Mo species has a strong impact on the catalytic performance.[8,10,13,17] During the past few years, the exact structures of the Mo species on zeolites have been extensively studied in MDA.

The structure of the Mo species supported on HZSM-5 with various calcination temperatures was investigated in detail by Iglesia *et al.*[18–20]. The results of their work indicate that the MoO_x species were mainly distributed on the external surface at a low temperature (~350 °C) and migrated into the zeolite channels between 500 and 700 °C. The ion exchange of the mononuclear MoOx species at the Brønsted acid sites (BASs) leads to the formation of dinuclear $[Mo_2O_5^{2+}]$ species, with the extraction of Al ions and the disappearance of the two BASs. The active MoC_x species were formed during the initial stages of methane conversion with the reduction of the $[Mo_2O_5^{2+}]$ species. However, the higher content of the MoO_x species over the external zeolite surface results in the formation of $(MoO_3)_n$ oligomers or $Al_2(MoO_4)_3$, which were identified as the main reason for the poor catalytic performance. Similar results were also observed by Tessonnier *et al.*[21,22] As evidenced, when the number of BASs is too low to adopt dinuclear $[Mo_2O_5^{2+}]$ species, the formation of $Al_2(MoO_4)_3$ or extra-framework $(MoO_3)_n$ cannot be avoided. The results of these works suggest that both the high dispersion of $[Mo_2O_5^{2+}]$ species inside the zeolite channels and the formation of MoC_x during the induction period are critical for methane conversion.

In the work performed by Kosinov *et al.*,[23] the structural and textural stability of the Mo/HZSM-5 catalyst was investigated as a function of the different Mo loadings. As shown in Fig. 1a and b, the low Mo/Al ratios lead to the dispersion of monomeric and dimeric Mo-oxo species in the zeolite micropores, even under an increased calcination temperature. Therefore, an almost unchanged catalytic performance with respect to the calcination temperature was observed for catalysts with low Mo loading contents (1–2 wt%). However, for Mo/HZSM-5 with a Mo loading of 5 wt%, the reaction of the Mo-oxo species with the framework Al causes the formation of $Al_2(MoO_4)_3$ and destroys the main framework of the zeolite, resulting in a rapid reduction of its initial activity. A similar conclusion was also demonstrated by Julian *et al.*[24] in Fig. 2a and b, that is, the catalyst with a low loading of 5% Mo on MCM-22 exhibited the best benzene selectivity and stability as compared to the samples with Mo loadings of 8% and 10%. With the application of *in situ* X-ray absorption spectroscopy (XAS), the impact of the Mo coordination environment in the MFI zeolites towards the MDA performance was recently systematically studied by Agote-Aran *et al.*[25]. As shown in Fig. 2c and d, when the calcination temperature is above 600 °C, the peaks for the Mo/Silicalite-1 in the post-edge region of the near edges spectra disappeared, along with the gradually decreased Mo–Mo peak intensity in the extended X-ray absorption fine structure (EXAFS), indicating the loss of the long-range order with the formation of Mo-oxo species in the microporous framework. By comparing with Mo/H-ZSM-5, the presence of BASs was found to be important for the stabilization of the Mo species, but not essential for benzene generation. The results from these works proved the dispersion of the MoO_x species as a key factor for improving the catalytic performance for methane conversion. In recent work performed by Julian *et al.*,[26] supercritical fluid was used to enhance the dispersion of Mo species within the zeolite channels. After 15 h MDA, the catalyst prepared under supercritical conditions revealed well dispersed MoC_x clusters at the zeolite surface, while carbon nanotubes and nanofibers were observed for the catalyst prepared using the conventional impregnation (IMP) method (Fig. 2e). Owing to the excellent Mo dispersion, the long-term catalytic stability of Mo/ZSM-5 was achieved and the formation of coke species on the Mo active sites was alleviated.

The Mo carbide species (such as Mo_2C and MoO_xC_y), formed from the reduction of the Mo species by methane during the reaction induction period, have generally been considered as active sites for methane activation. The induction period in MDA over Mo/HZSM-5 was first mentioned in the work conducted by Lunsford *et al.*[27] The results of this work suggest that the Mo^{6+} species are reduced to Mo_2C during the induction period. In addition, compared to the clean surface of Mo_2C, which is too reactive for the formation of higher hydrocarbons, the coke modified Mo_2C was identified as being critical for the formation of ethylene.[28] Further studies indicate that the Mo species on the external surface of the zeolite could be easily reduced to β-Mo_2C, and it is partially transformed to MoO_xC_y in the zeolite channels, which was identified to be critical for the MDA.[29] Taking advantage of the operando time-resolved combined X-ray diffraction (XRD) and X-ray absorption near-edge spectroscopy (XANES), Beale *et al.* demonstrated that the metastable MoO_xC_y species converted from Mo-oxo species are primarily responsible for the formation of C_2H_x/C_3H_x.[30] Recently, thermochemical kinetic analyses were employed by

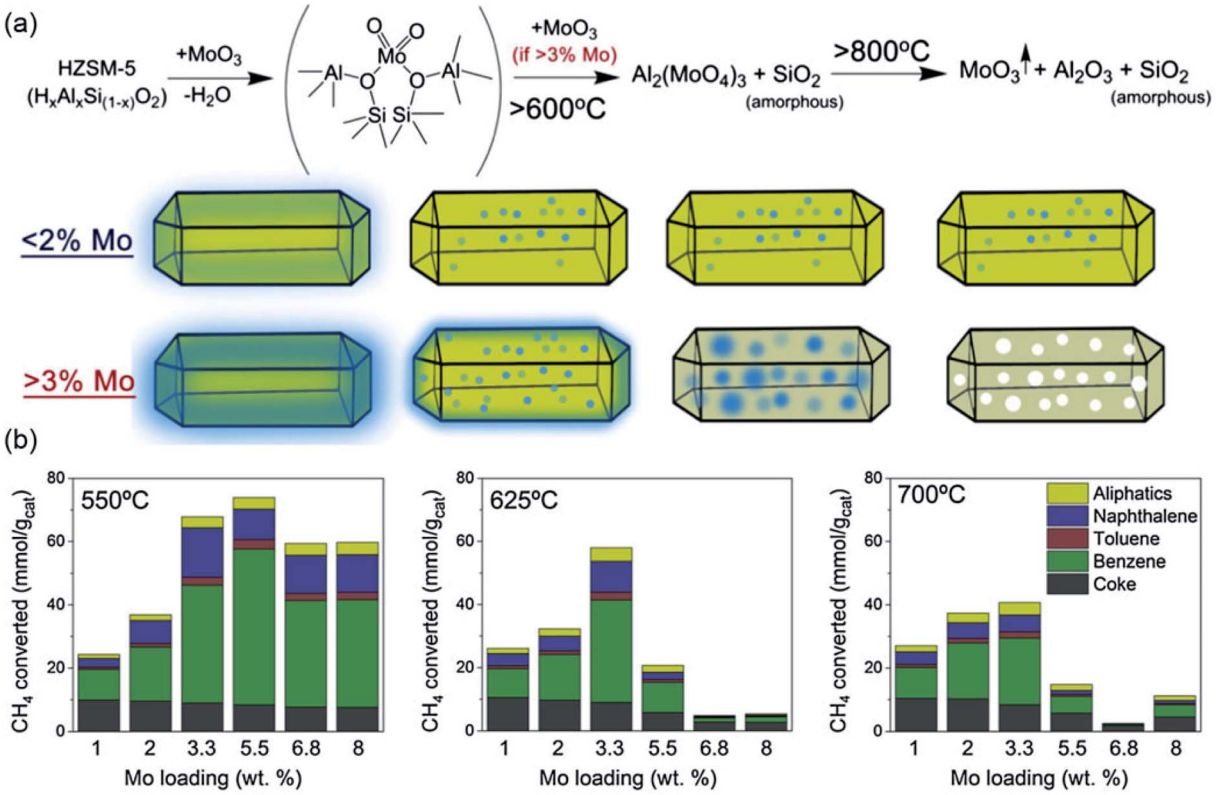

Fig. 1 (a) Schematic representation of the dispersed monomeric and dimeric Mo-oxo species in the MoO_3-HZSM-5 catalysts. (b) Cumulative product yields of the Mo/HZSM-5 catalysts pre-calcined at different temperatures during 16 h MDA tests. Reproduced with permission from ref. 23. Copyright 2017 Elsevier.

Bhan *et al.*[31] to ascertain the catalytic roles of the BASs and Mo carbide species. The results of this work suggest that the active carbidic Mo content is the only catalyst descriptor that can be used to predict the steady state and activity of MDA catalysis over Mo/HZSM-5, while the zeolitic acid sites were found to be beneficial for dispersing Mo species to catalyze the equilibrated reaction steps. In the work conducted by Rahman *et al.*,[32] the catalytic activity and stability over MoC_y/HZSM-5, with *ex situ* prepared Mo carbides, was found to be much higher than that of MoO_x/HZSM-5. All of these works highlight the critical role of BASs and Mo carbide species in MDA. However, to avoid the formation of $Al_2(MoO_4)_3$ and extra-framework (MoO_3) species, the optimal contents of BASs and Mo carbide species should be considered in future studies.

A bifunctional mechanism, including the conversion of methane into ethylene on Mo carbide sites and subsequent oligomerization into aromatics over BASs, has been widely proposed for the Mo/zeolites catalytic systems.[33] However, the mechanism emphasized both the activation of methane to acetylene and the subsequent aromatization over the Mo carbide phase have also been reported in many previously published works.[18,34,35] In addition, the Mo-based carbide plays an important role in the C–H activation and C–C coupling to C2 intermediates. Theoretically, we have performed a systematic study of the methane activation and conversion over the Mo-terminated surfaces derived from different phases of the Mo_2C carbides (Fig. 3). Our results show that Mo-terminated orthorhombic β-Mo_2C, with a lower carburization in its subsurface, possesses a superior reactivity toward methane C–H activation, resulting in the complete dissociation of methane to the carbon adatom on the surface. This carbon adatom causes further carburization of the surface, reducing the reactivity toward methane activation.[36] Moreover, although carburization reduces the activities for methane activation, it promotes C–C coupling for dimerization of the $(CH)_{ad}$ species, resulting in $(C_2H_2)_{ad}$ on the Mo-terminated surfaces. On the deep carburized molybdenum carbide (MoC) surfaces, the Mo-terminated MoC surfaces derived from different bulk phases (hexagonal α-MoC and cubic δ-MoC) of MoC possess a similar mechanism to that on the noble-metal surfaces for methane dissociation, that is, CH_4 dissociates sequentially to $(CH)_{ad}$ with both kinetic and thermodynamic feasibilities while breaking the last C–H bond in $(CH)_{ad}$ requires a high activation barrier. As such, C–C coupling through dimerization of the $(CH)_{ad}$ species occurs more readily, resulting in $(C_2H_2)_{ad}$ on the Mo-terminated surfaces. These $(C_2H_2)_{ad}$ species can dehydrogenate easily to other C2 adsorbates such as $(C_2H)_{ad}$ and $(C_2)_{ad}$. Consequently, these C2 species from CH_4 dissociation will likely be precursors for producing long chain hydrocarbons and/or aromatics on molybdenum carbide based catalysts or oligomerization over BASs.[37]

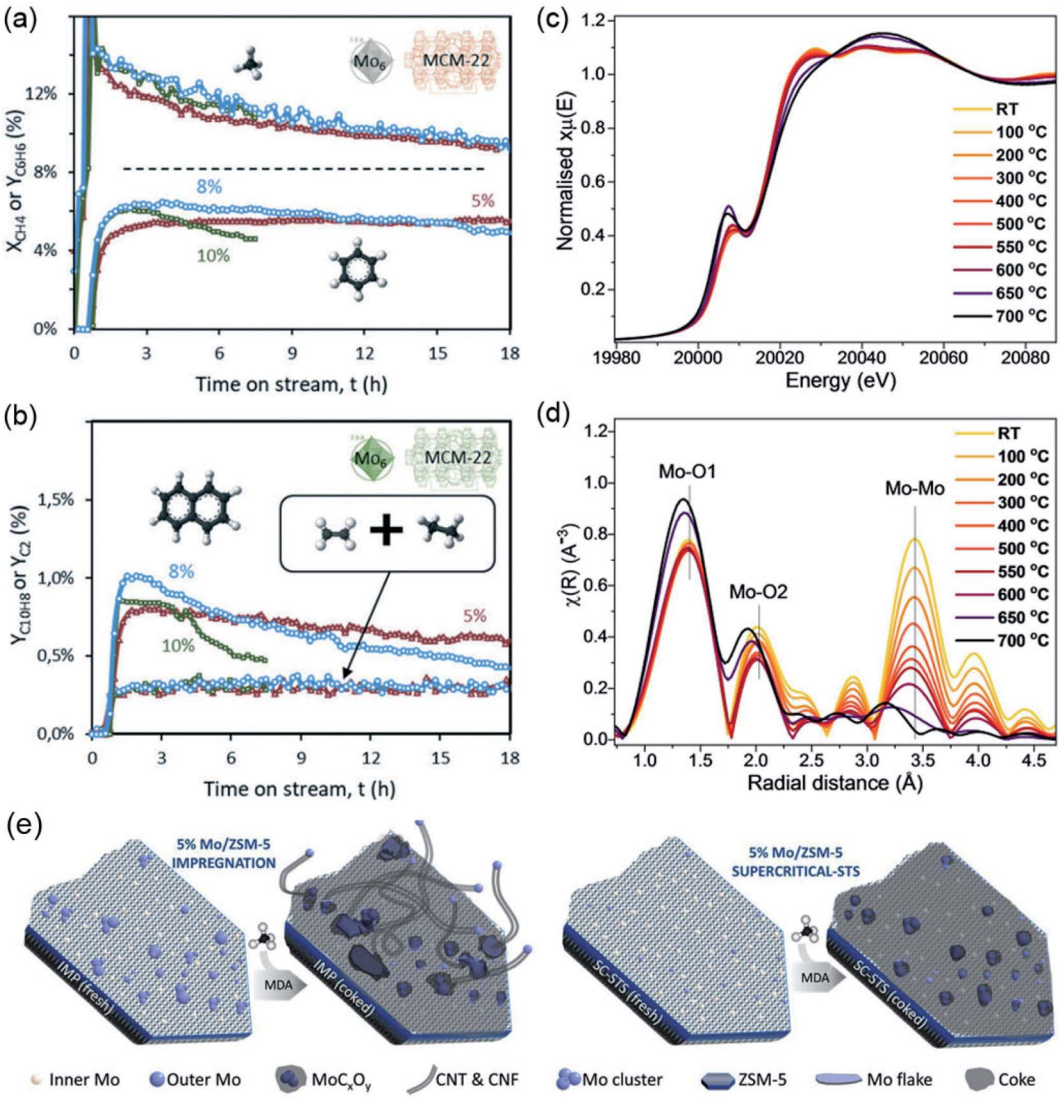

Fig. 2 (a) Transient benzene yield, (b) naphthalene and C2 (ethane, ethylene) yield obtained for the Mo/MCM-22 catalysts with different Mo loadings. Reproduced with permission from ref. 24. Copyright 2019 Royal Society of Chemistry. (c) XANES spectra, and (d) FT-EXAFS of Mo/silicalite-1 collected during *in situ* calcination. Reproduced with permission from ref. 25. Copyright 2020 John Wiley and Sons. (e) Conceptual drawing of the distribution of Mo species for fresh and spent Mo/ZSM-5 prepared using different methods. Reproduced with permission from ref. 26. Copyright 2020 Elsevier.

2.1.2 Influence of the structural feature of zeolites. Zeolites are porous, three-dimensional crystalline solids with well-defined structures built from interlinked tetrahedra of silica (SiO_4) and alumina (AlO_4). They have been extensively used as catalyst supports for methane conversion owing to their large surface area, thermal stability, as well as the presence of Brønsted acid sites. Among the different types of zeolites, H type silica-alumina zeolites (HMCM-49, HZSM-5 and *etc.*) have been evidenced as the most suitable supports for MDA catalysts owing to their porous structure with pore diameters close to the dynamic diameter of benzene molecules.[38] Accordingly, the influence of structural features including the Si/Al molar ratio, the strength and density of BASs, as well as the pore architecture of the zeolite supports on the catalytic performance have been widely explored.

It is generally agreed that the BASs plays an important role in MDA, which serve as both the anchoring centers for the metal species and oligomerization sites for C_2H_x to benzene or coke.[39,40] The strength and density of the BASs, which are related to the Si/Al ratio and pore architecture of the zeolite supports, thus determine the location and nature of the Mo species, as well as the overall catalytic performance. For instance, the partial removal of the framework Al from the zeolite lattice, with decreases in both the strength and number of BASs, results in a noticeable improvement in the benzene yield and the durability of the catalyst for the Mo/HZSM-5 catalyst.[41] A recent study conducted by Kosinov *et al.* suggests that the embedding of the Mo oxide into properly sized micropores is critical for the conversion of methane into benzene (Fig. 4a), and the role of BASs in promoting the dispersion of Mo species.[34] In addition,

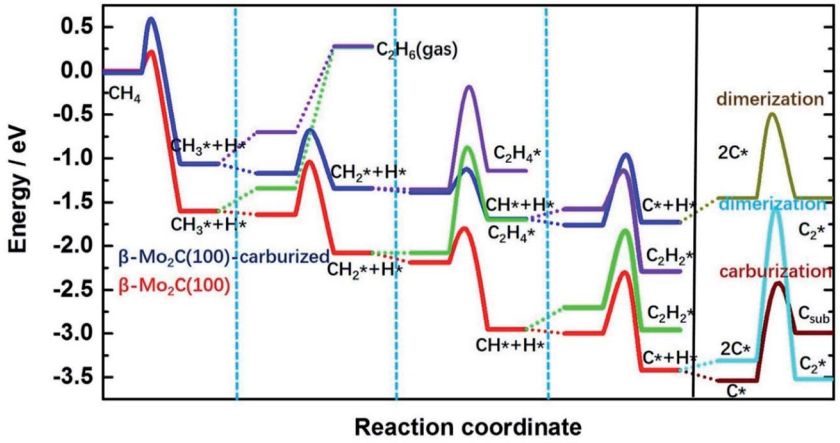

Fig. 3 Energy profile of the elementary steps for methane dissociation, the dimerization of CH_x* species and the carburization on carburized β-Mo_2C(100) surfaces. Reproduced with permission from ref. 36. Copyright 2020 Elsevier.

by varying the ratios of Si/Al_2, monomeric Mo oxide species could be stabilized on the MCM-22 zeolite as a result of the promoted migration of Mo oxides into the micropore (Fig. 4b). The microchannels of the zeolite were observed to be critical for providing a shape-selective environment, thus enhancing the rate of benzene formation.[42] The effect of the Si/Al ratio on the activity of the Mo/HZSM-5 catalysts was further studied by Rahman *et al.*,[43] and their results indicate that a higher channel occupation of Mo species, resulting from a lower Si/Al ratio and higher Mo loading over HZSM-5 zeolite, is directly correlated with the higher selectivity and yield towards benzene. In the work performed by Tan *et al.*,[44] by impregnating the HZSM-5 zeolite with NH_3 heptamolybdate solution, the catalytic performance of Mo/HZSM-5 was significantly improved owing to the larger amount of highly dispersed Mo species on the HZSM-5 zeolite.

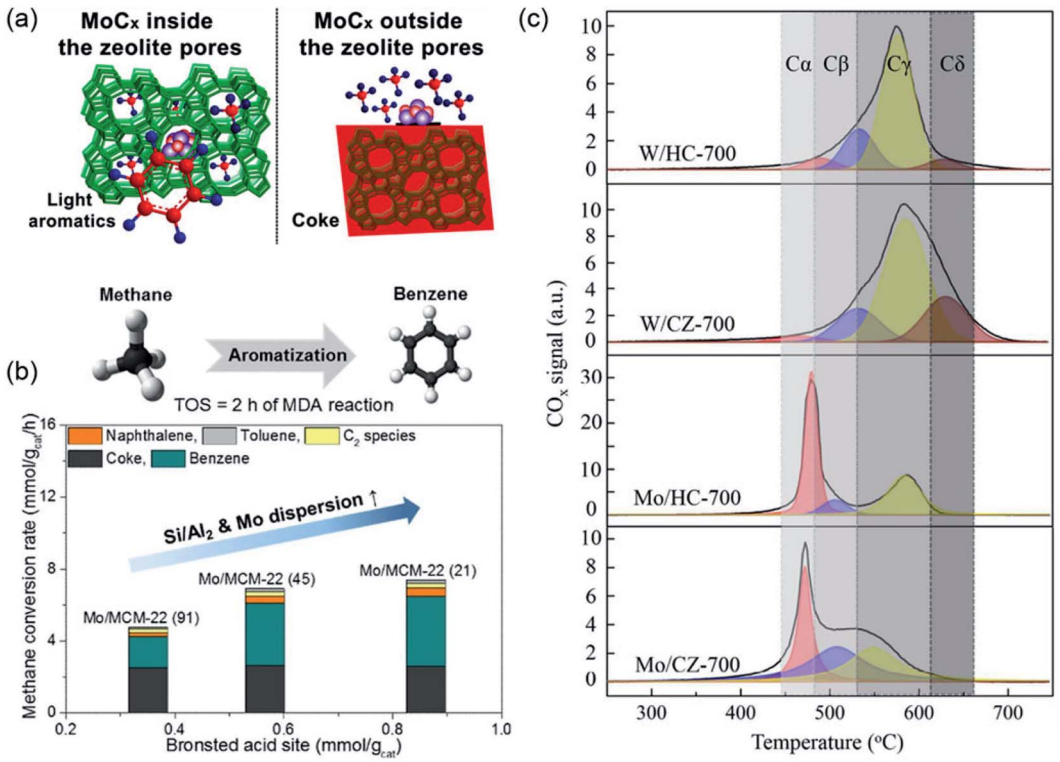

Fig. 4 (a) Mo carbide dispersed inside and outside of the zeolite pores for MDA. Reproduced with permission from ref. 34, Copyright 2016 American Chemical Society. (b) Effect of Si/Al_2 ratios in Mo/H-MCM-22 on MDA. Reproduced with permission from ref. 42, Copyright 2018 Elsevier. (c) Gaussian deconvolution of the TPO profiles for a metal supported on a hollow capsule (HC) or commercial HZSM-5 (CZ). Reproduced with permission from ref. 46, Copyright 2018 Royal Society of Chemistry.

The cooperative effects of the zeolite structure and metal species also affect the catalytic performance for MDA. For instance, a hollow silicalite-1-HZSM-5 zeolite with a capsule structure as a support for Mo nanoparticles (Mo/HZSM-5) was developed by Zhu *et al.*[45]. The hollow structure of the zeolite was suggested to accelerate the mass-transfer rate, which significantly improved the rate of benzene formation and the catalytic stability. Recently, in the work performed by Huang *et al.*,[46] a hollow HZSM-5 capsule zeolite (HC) was prepared and used as the MDA supports. As shown in Fig. 4c, the different coke types were clearly discriminated, which depend greatly on the structure of the zeolites and the metals, and the hollow capsule structure is important for suppressing the external coke (Cβ) formation in Mo-based catalysts (Mo/HC-700), leading to an excellent catalytic stability in the MDA reaction.

2.1.3 Effect of the promoters. A number of investigations have been carried out to improve the catalytic performance of Mo/zeolite catalysts by introducing other metals as promoters.[8] Among all these metal promoters, Fe, Mg, Cr, Co, Ni and K have been widely studied and have shown an improved catalytic activity, stability, and selectivity to aromatics.[10,47–49] Recent studies indicate that the promoters are beneficial for increasing the amount of active Mo species and reducing the formation of coke in zeolite channels, thus enhancing the catalytic performance for CH_4 conversion.

In work reported by Cheng *et al.*,[50] a series of metal modified Mo/ZSM-5 were prepared as MDA catalysts. With Mg as a promoter, both the catalytic activity and selectivity to benzene were improved with an inhibited carbon deposition. X-ray photoelectron spectroscopy results demonstrated that the promotion effect in generating Mo_2C active species by the presence of Mg was the main reason for the improved catalytic performance. Recently, Sridhar *et al.* found that with modification using Co and Ni additives, Zeolite-supported Mo carbide catalysts could increase the yield of benzene along with a better stability.[51] However, the effect of the additives was only beneficial for catalysts with *ex situ* formed Mo carbide species by pre-carburization. As shown in Fig. 5, the MoO_3 peak completely disappeared with the appearance of Mo_2C as the active phase for the spent catalysts pre-treated using helium. With Co- and Ni-modification, a much stronger Mo_2C peak was observed for the pre-carburized catalysts, indicating sintering of the Mo_2C phases over the external surface of the zeolite. The synergy effect between the additive and Mo thus changed both the reducibility and mobility of the Mo species, which increases the retention of the Mo species within the channels of zeolite and benefits the catalytic selectivity towards benzene.

The addition of metal promoters is also beneficial for reducing the formation of coke in zeolite channels. For instance, in the work performed by Bajec *et al.*,[52] the addition of

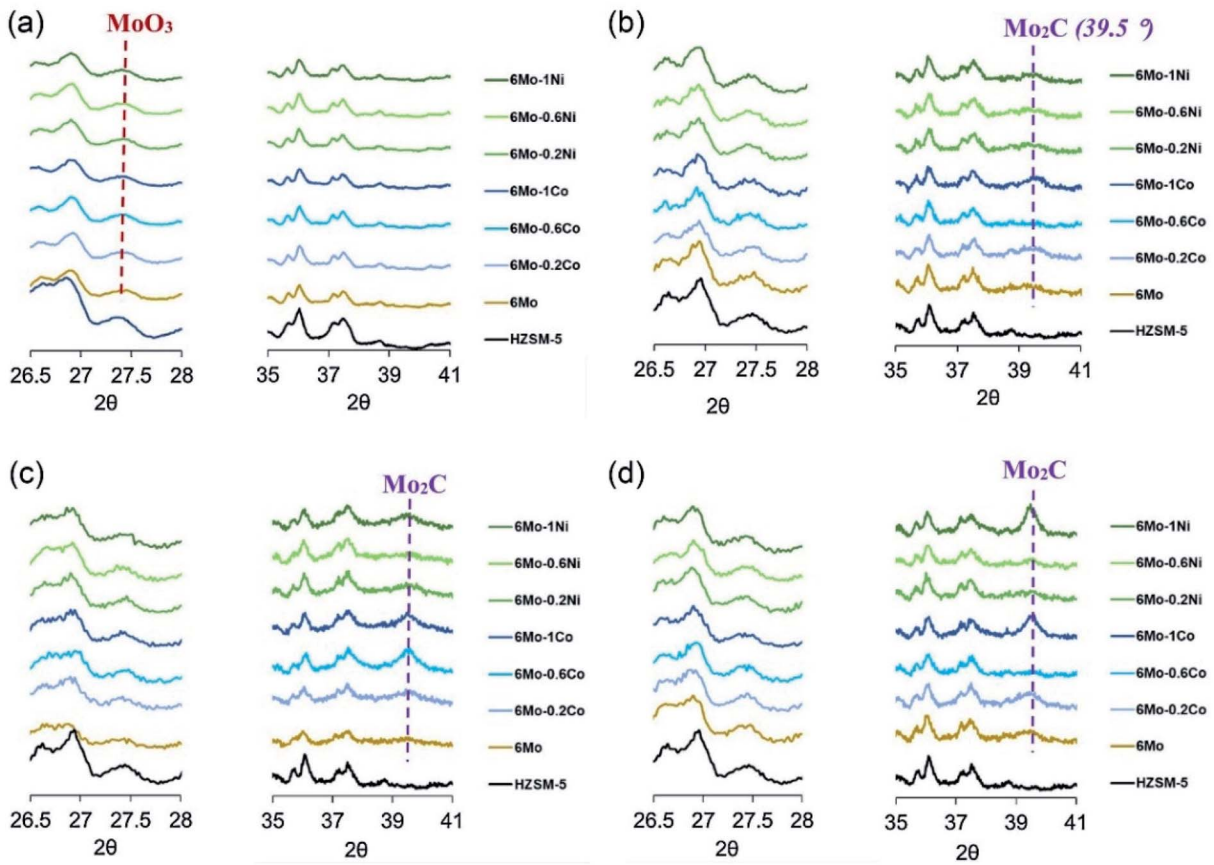

Fig. 5 XRD patterns for (a) He pre-treated, (b) pre-carburized, (c) spent He pre-treated and (d) spent pre-carburized Co- and Ni-modified Ni/ZSM-5 catalysts. Reproduced with permission from ref. 51. Copyright 2019 Elsevier.

Fe to Mo/HZSM-5 catalysts reduces the amount of coke formation, which results in a better stability for the coupling of methane to ethane/ethylene synthesis. The effect of the addition of Fe, Rh, and K on MDA over Mo/HZSM-5 was studied by Ramasubramanian *et al.*,[53] in which the K-promoted catalyst was found to have a better selectivity for benzene (~50%) after 255 min of reaction (Fig. 6a). The temperature programmed oxidation results (Fig. 6b) indicated that the formation of coke was largely reduced by the addition of K, which modified the acidic strength of Mo/HZSM-5 and restricted the agglomeration of C_6H_6 to coke. Recently, the promoting effect of nano-Fe on the MDA performance over the Mo/HZSM-5 catalyst was studied by Sun *et al.*,[49] and a mechanism for the formation of carbon nanotubes was suggested during the nonoxide dehydroaromatization. In their proposed mechanism, the coke formation over both the external surfaces and channels of zeolite could be suppressed owing to the competitive consumption of coke precursors by the formation of carbon nanotubes over nano-Fe. Meanwhile, these carbon nanotubes created by Fe lead to appropriate cavities with a kinetic diameter of about 10.0 Å. The activation of methane was speculated to facilely occur over the Brønsted sites inside the carbon nanotubes, thus enhancing both the rate and stability for the production of aromatics.

2.2 Non-Mo based catalysts

In addition to the studies on Mo-based catalysts, non-Mo based catalysts such as Pt-containing catalysts, transition metals (Fe, Zn, Cr, Ni, Cu, and Co) and metals in group IIIB (Ga and Al) supported on SiO_2 and H-ZSM-5 have also been extensively investigated to enable improved catalytic activity and stability for methane activation and conversion.

2.2.1 Pt-containing catalysts. The early work by Belgued *et al.* reported that the conversion of methane to higher hydrocarbon products over a 6 wt% Pt/SiO_2 catalyst occurs at a reaction temperature of 250 °C[54] which is even lower than that for the OCM, while it suffered from a low methane conversion rate. In the work conducted by Dumesic *et al.*,[55] PtSn bimetallic catalysts supported on a H-ZSM-5 zeolite were developed to improve the activity and selectivity of nonoxidative methane conversion. As shown in Fig. 7a, the addition of Sn to Pt/SiO_2 was found to be beneficial for ethylene formation. By varying the acidity of the H-ZSM-5 support, the selectivity to benzene and naphthalene can be realized *via* the oligomerization of C_2H_x intermediates. The bimetallic and stepped surfaces of the Pt and PtSn surfaces were shown to be critical for higher rates of ethylene formation. In addition, Varma *et al.*[56] recently reported that bimetallic Pt–Bi supported on ZSM-5 zeolite could afford a stable methane conversion with a selectivity of more than 90% to C2 species at relatively moderate temperatures (Fig. 7b), and the surface Pt was found to be the active site for methane activation while the addition of Bi plays an important role in catalyst stability and selectivity to C2 species.

2.2.2 Ta-based catalysts. Silica-supported tantalum hydride $(\equiv SiO)_2Ta–H$ is known to catalyze the hydrogenolysis of ethane into methane. Basset *et al.* reported the first example of the transformation of methane into ethane *via* nonoxidative coupling[57] over a heterogeneous Ta-based catalyst $(\equiv SiO)_2Ta–H$. A high selectivity (>98%) of ethane was achieved among the hydrocarbon products with a methane conversion degree of approximately 0.1% at a temperature of 375 °C in the continuous flow reactor. As shown in Fig. 8a, the reaction mechanism involved the migration of the methyl ligand onto tantalum-methylidene, which was proposed as the key intermediate for ethane formation in the NOCM. Recently, free $Ta_8O_2^+$ cluster ions were also found to be capable of NOCM reactions.[58] A similar catalytic cycle for the C–C coupling step was proposed on the $Ta_8O_2^+$ cluster ions and the Ta-based catalyst (Fig. 8b), and the difference lies in the final step of the product formation. As shown in Fig. 8c, the activation of an extra methane molecule was required for the formation of ethane over tantalum hydride catalysts, while the formation of ethane was completed with the previously formed carbene and methane on $Ta_8O_2^+$. The results of these works prove the great potential of tantalum-based catalysts for the NOCM.

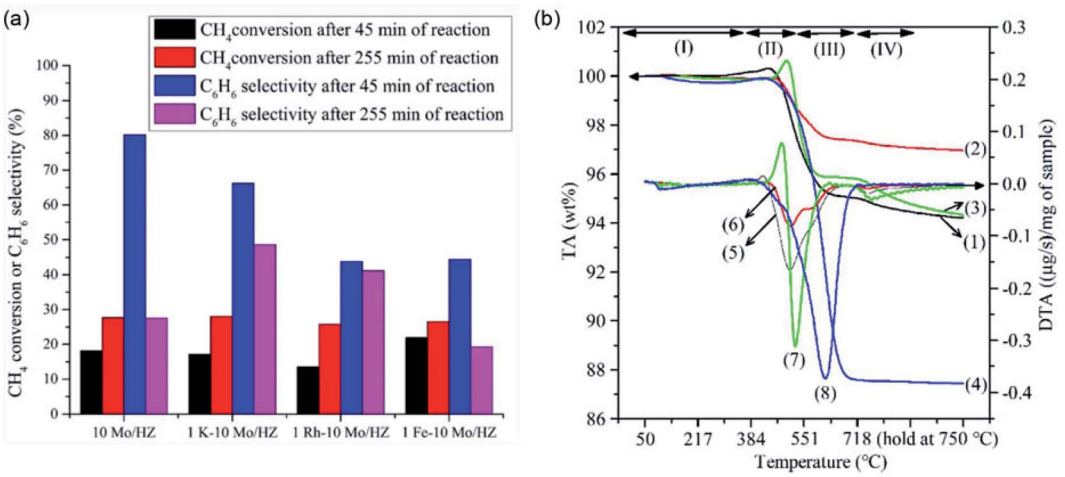

Fig. 6 (a) Effect of addition of Fe, Rh, and K on MDA over Mo/HZSM-5. (b) TPO profiles of Rh (green line), Fe (blue line), and K (red line) promoted, as well as parent (black line), Mo/HZSM-5 catalysts. Reproduced with permission from ref. 53. Copyright 2019 Springer.

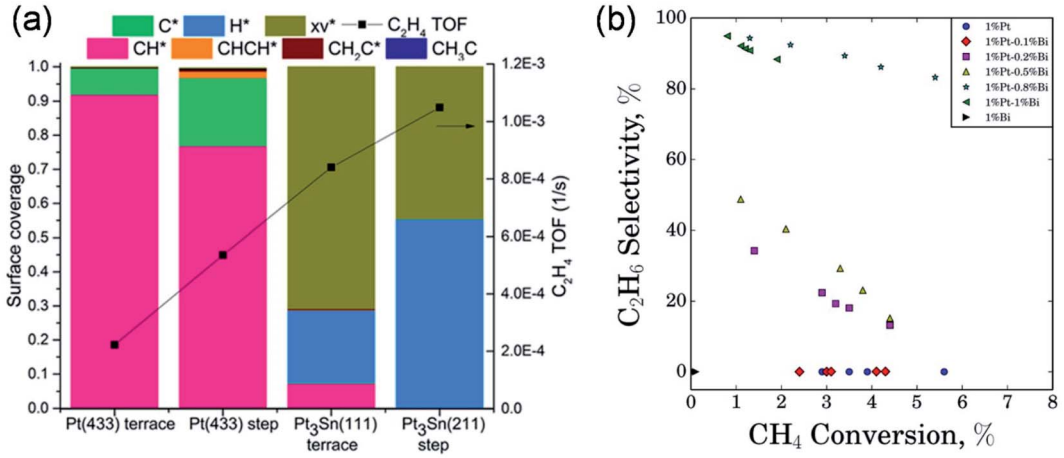

Fig. 7 (a) Surface coverage and ethylene turnover frequency values of the PtSn/H-ZSM-5 surfaces under conditions of 5% H_2 cofeeding with methane predicted using the microkinetic model. Reproduced with permission from ref. 55. Copyright 2017 American Chemical Society. (b) Performance of different Pt–Bi/ZSM-5 catalysts at various methane conversions for ethane selectivity over ZSM-5 zeolite supported bimetallic Pt–Bi catalysts. Reproduced with permission from ref. 56. Copyright 2018 American Chemical Society.

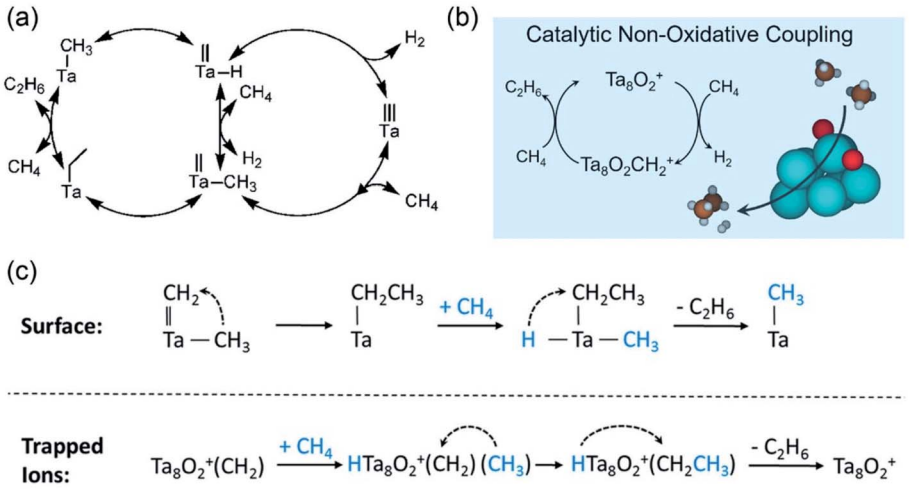

Fig. 8 (a) Proposed mechanism for NOCM over silica-supported tantalum hydride $(\equiv SiO)_2Ta-H$. Reproduced with permission from ref. 57. Copyright 2008 American Chemical Society. (b) NOCM catalyzed by $Ta_8O_2^+$. (c) Comparison of the mechanisms for ethane formation in NOCM. Reproduced with permission from ref. 58. Copyright 2020 American Chemical Society.

2.2.3 Ga-modified zeolites. The concept of Ga-modified zeolites for methane conversion was based on consideration of the Ga species serving as the active centers for both methane activation and dehydrogenation. By using gas chromatography mass spectrometry (GC-MS) analysis and ^{13}C solid-state NMR spectroscopy, Ga-methyl species derived from the dissociative adsorption of methane on Ga_2O_3 species were identified as the major intermediates in methane activation.[59] These Ga-methyl species can then enable nucleophilic substitution in the aromatic ring, which thus provides an alternative pathway for NOCM. Kopyscinski *et al.* recently developed GaN/SBA-15 catalysts for direct NOCM to ethylene,[60] and the catalytic results indicated that the Ga-nitrides exhibited a higher ethylene selectivity (71%) and a reduced coke selectivity (27%) as compared to those of the oxide precursors. In their further work, the regeneration capabilities of the GaN catalysts were also studied.[61] As shown in Fig. 9, the surface Ga_2O_3 layer can be converted to GaN (step R8) by the renitridation step using NH_3, to maintain its capability for ethylene production.

2.2.4 Zn-Modified catalysts. Zn-Modified zeolites for the conversion of light alkanes have also attracted significant attention owing to the proven evidence of their good catalytic capability.[62,63] The key factor in determining the high activity of Zn-modified zeolites is considered as the initial stage of methane activation. With Zn-modified H-BEA catalysts, the mechanism of methane activation was proposed *via* heterotypic C–H bond cleavage by the formation of methoxy species on the surface.[64] Similar results were also observed for methane activation over the Zn-modified H-ZSM-5 zeolite.[65] The nature of the Zn species, for example, ZnO clusters or isolated Zn^{2+}, has

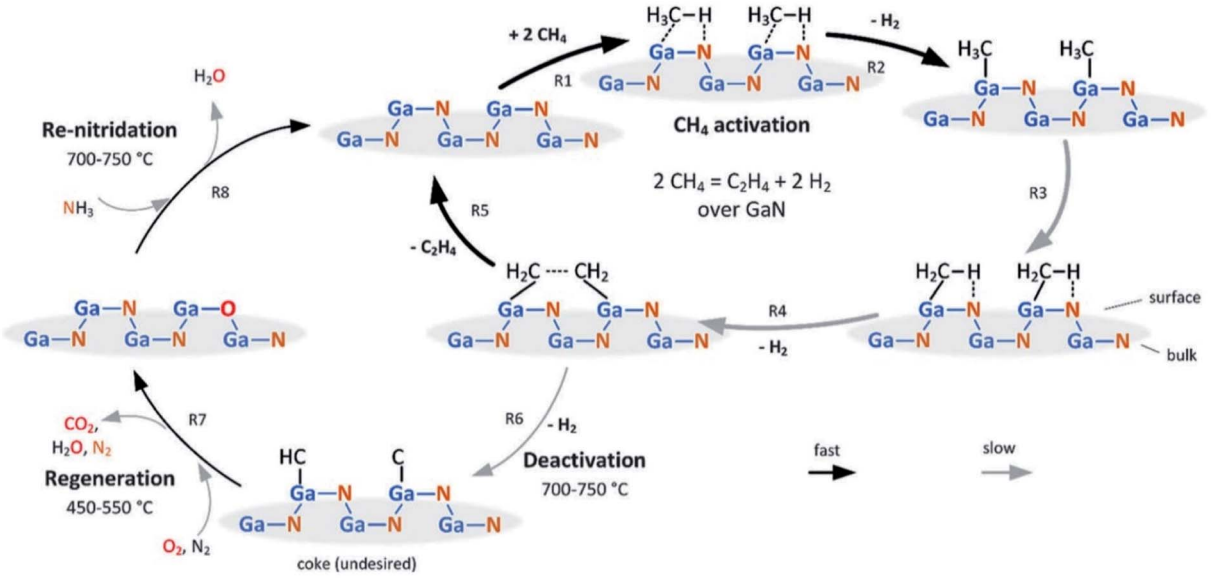

Fig. 9 Proposed mechanism for the activation/regeneration/renitridation cycle of GaN/SBA-15 in NOCM. Reproduced with permission from ref. 61. Copyright 2020 American Chemical Society.

a significant impact on the catalytic efficiency towards methane activation, and isolated Zn^{2+} species demonstrate a better performance.[66] In the work conducted by Gabrienko *et al.*,[67] the methane conversion catalyzed by Zn^{2+} exchanged H-ZSM-5 zeolite was studied using ^{13}C magic angle spinning (MAS) NMR spectroscopy. They suggested that the methane activation under nonoxidative conditions occurs on the zinc cationic sites through the "alkyl" pathway by forming Zn–CH_3 species. The BASs on the zeolite take part in the formation of zinc-methyl species, indicating the involvement of both Zn sites and BASs for NOCM on Zn^{2+}/H-ZSM-5. This synergic mechanism between the BSAs and Zn^{2+} ions in zinc-modified ZSM-5 zeolites was further confirmed by Qi *et al.* by using ^{1}H–^{67}Zn double-resonance solid-state NMR spectroscopy.[68] As shown in Fig. 10a, owing to dipolar interactions between the Zn species and protons, the ^{1}H signals from SiOH, ZnOH, and SiOHAl can be well distinguished. The degree of ^{1}H–^{67}Zn dipolar dephasing, expressed as $\Delta S/S_0$ (Fig. 10b), indicated the different degrees of dipolar interaction between the three hydroxy groups and Zn atoms. The spatial proximity/interaction between the BASs and Zn^{2+} ions with the enhanced Brønsted acidity was suggested as the main cause for the promotion of C–H bond activation on the Zn^{2+} ions.

The co-aromatization mechanism of methane with other hydrocarbons on Zn-modified zeolites has also been widely explored. It is proposed that methane was first converted to a methoxy species when co-fed with higher hydrocarbons. By undergoing methyl formation with the aid of aromatic species in the zeolite, it was then transferred to the phenyl rings.[64] Recently, He *et al.* studied the impact of the Al sites of Zn/HZSM-5 on the methane conversion mechanism during the co-aromatization with alkanes.[69] The diffuse reflectance infrared Fourier transform spectroscopy (DRIFTS) and NH_3-TPD characterization results of Zn/HZSM-5 suggest that the extra-framework and framework Al sites are related to the Lewis acid and Brönsted acid of the zeolite, respectively. Both the extra-framework and framework Al sites were demonstrated to be vital for methane activation, and the catalytic activity could be enhanced by converting some of the framework Al atoms to the extra-framework Al sites. Meanwhile, the effect of the Zn location in Zn/HZSM-5 was also studied for the co-aromatization of methane/alkanes, in which the Zn species located on the external surface of HZSM-5 were related to the generation of the alkyl substitution group while the Zn within the inner pores was responsible for the formation of the phenyl rings of the aromatics.

2.2.5 Fe-modified catalysts. Among the various transition-metal-based materials, the Fe-based catalyst has been extensively used in NOCM owing to its abundant and environmentally friendly nature. Extensive studies have been carried out to identify the real active phases of iron for methane activation. In the work conducted by Weckhuysen *et al.*,[70] the 2 wt% Fe_2O_3/HZSM-5 catalyst, after activation in CO or O_2 at 500 °C, achieves an approximately 4.2% conversion of methane with a selectivity of approximately 70% to benzene. The iron suboxides, which are located on the external surface of the HZSM-5 and formed from the reduction of Fe_2O_3 by methane, were supposed to be the active phases for methane activation.[71] In addition, studies of Fe_2O_3 on Al_2O_3 and SiO_2 showed that the Fe_2O_3 phase transformed into Fe_3C and metallic Fe saturated with carbon atoms during methane decomposition.[72] Furthermore, these carburized Fe and metallic Fe were found to be highly effective for methane activation to aromatics and were also reported to be carbonaceous in work performed by Tan *et al.*[73]. It was proposed that the carburized Fe serves as the active species to stabilize the carbene *via* the formation of a metal-carbene complex (C–Fe=CH_2), which dimerizes into ethylene and is then oligomerized into the aromatics on the acid sites of the

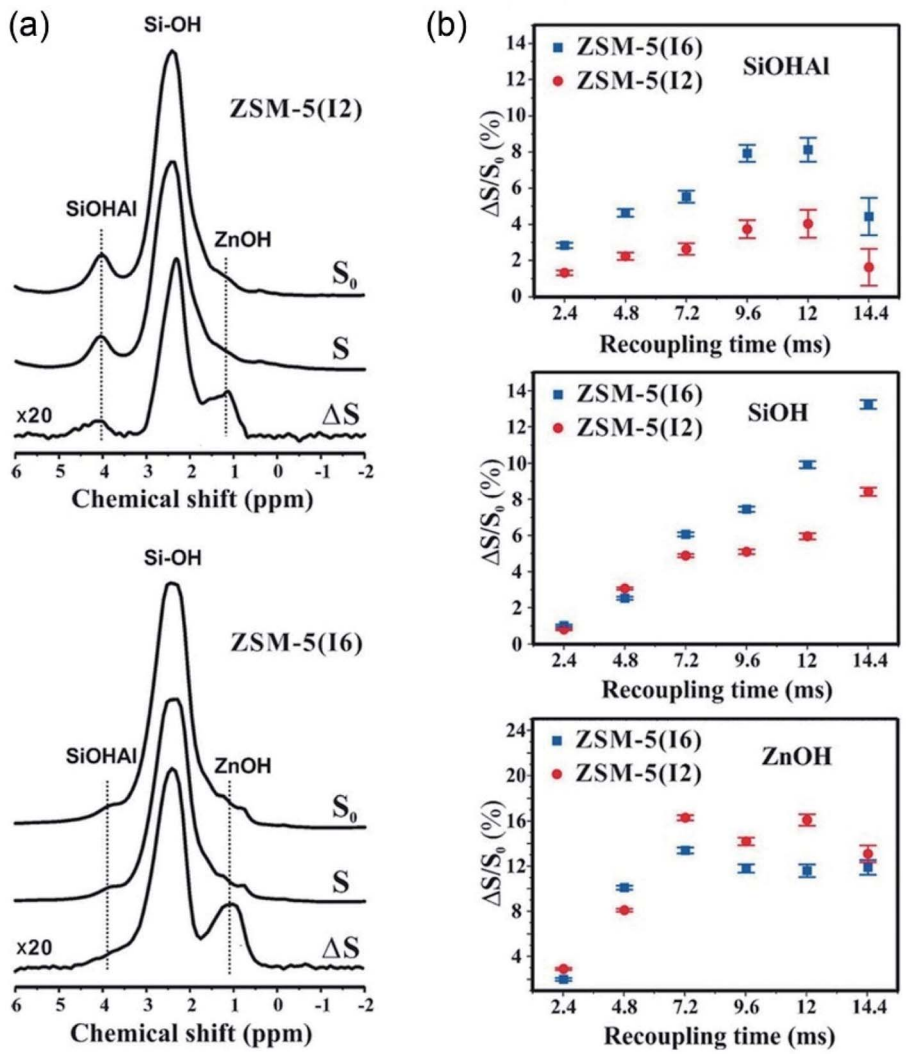

Fig. 10 (a) NMR spectra of ZSM-5(I2) and ZSM-5(I6) recorded at 18.8 T with a recoupling time of 9.6 ms. (b) $\Delta S/S_0$ signal fraction *versus* the total recoupling time. S and S_0 denote the ^{1}H spectrum with and without ^{67}Zn irradiation, respectively. Reproduced with permission from ref. 68. Copyright 2016 John Wiley and Sons.

zeolite. On the other hand, the degree of carburization of the Fe species can be enhanced in the presence of promoters, which promote the reactivity of NOCM over the Fe-based catalyst. For example, the promotional effect of Au toward the carburization of Fe on Fe/HZSM-5 for an improved NOCM was recently reported by Sim *et al.*[74].

3. Newly developed single-atom based catalysts

A single-atom catalyst (SAC), defined as a catalyst composed of only isolated single atom active sites on supports,[75] provides significant advantages for optimizing the catalytic performance owing to the well-defined structure of the catalytic sites. Even though highly dispersed Fe cations supported on HZSM-5 were shown to be active in the NOCM, they suffered from severe coke deposition.[73,76,77] Novel catalytic systems are thus greatly desired to make the nonoxidative conversion of methane more selective and efficient. In this regard, coordinatively unsaturated iron sites show significant potential owing to their high activity towards C–H activation.[78,79] In 2014, Bao and colleagues reported single iron atoms embedded in the lattice of silica (Fe@SiO_2) as a highly efficient catalyst for the nonoxidative conversion of methane to ethylene and benzene (Fig. 11a).[15] As shown in Fig. 11b and c, these coordinatively unsaturated iron atom species interact extensively with the SiO_2 through bonding to the Si and C atoms, leading to an excellent stability, even after a prolonged reaction time of 60 h. This study was viewed as a landmark discovery for the transformation of methane, and it thus opened up a new avenue for the application of single atom catalysts (SACs) in NOCM.

Over the past few years, a number of studies have been carried out using SACs as catalysts for NOCM.[80–85] For instance, the effect of the catalytic surface of silica-based iron catalysts (Fe©CRS) on MTOAH was studied by Han *et al.*[81]. The highly

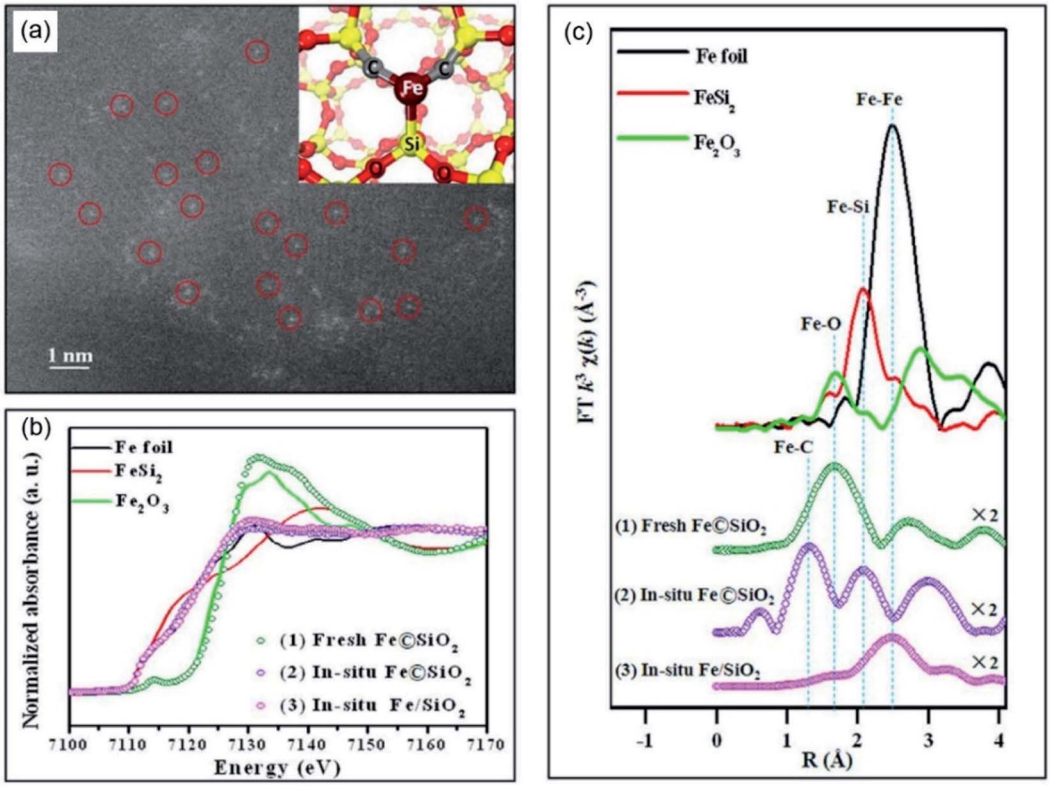

Fig. 11 (a) Scanning transmission electron microscopy high-angle annular dark-field (STEM-HAADF) image of Fe@SiO_2 (inset shows the computational model of single iron atoms embedded in the lattice of silica). (b) *In situ* XANES, and (c) Fourier transformed (FT) EXAFS spectra upon activation. Reproduced with permission from ref. 15. Copyright 2014, American Association for the Advancement of Science.

dispersed confined Fe sites with Fe–Si coordination were identified to be more favorable for the formation of the methyl radical compared to the Fe_3C clusters, and the optimized Fe©CRS catalyst can achieve a 6.9–5.8% methane conversion with a 86.2% C2 selectivity at 1080 °C for 100 h. Recently, nanoceria-supported single Pt atom catalysts (Pt_1@CeO_2) were demonstrated with a higher C2 product selectivity than that of Fe@SiO_2 at 950 °C.[85] Based on the DRIFTS analysis results, the methane conversion over Fe@SiO_2 was proposed through catalytic coupling of dehydrogenated *CH_3 and *CH_2 adsorbates on the single Pt sites. In the work carried out by Sakbodin *et al.*,[82] a significant improvement in methane conversion (~30% C_{2+} single-pass yield with 99% selectivity to C2 products at 30% methane conversion) was achieved by integrating the Fe@SiO_2 catalyst in a hydrogen (H_2) permeable tubular membrane reactor. A comparison of the catalytic performance for recently reported catalysts for the NOCM is shown in Table 1. As shown, the results from recent advances have demonstrated the isolation of single-Fe-atom sites as a promising way to maintain the catalytic activity and long-term stability, enabling more sophisticated studies to be performed to elucidate the underlying mechanism and optimize the catalysts, and even improve the design of the reactor to achieve an optimized performance for the NOCM.

On the other hand, considerable efforts have also been devoted to uncovering the catalytic mechanism of the NOCM on SACs. Results from recent theoretical studies provided an in-depth mechanistic understanding of the elementary steps.[86–90] In the work conducted by Bao and colleagues,[15] a gas-phase reaction mechanism was proposed based on preliminary theoretical calculations and VUV-SPI-MBMS analysis. It was proposed that methane was first activated over the single Fe atom center, resulting in the C–H bond cleavage of CH_4 with the dissociated H and methyl being adsorbed at the C and Fe sites, respectively. The target ethylene and aromatics were then generated from the released gas phase of methyl *via* gas-phase radical/molecule collision. Further quantum chemistry calculations performed by He *et al.* suggest a monofunctional mechanism occurs over the surface of the Fe@SiO_2 catalysts and metal/zeolites for the NOCM.[35] It was suggested in this work that both the activation of methane and its further C–C coupling occurred on the active FeC_3^- cluster. Recently, by using DFT calculation methods and *ab initio* molecular dynamics (AIMD) simulations, we have also systematically studied the reaction mechanisms of methane conversion over Fe_1@SiC_2.[87] As shown in Fig. 12a, a new quasi Mars–van Krevelen mechanism is revealed for NOCM over the Fe_1@SiC_2 active center. The activation of the C–H bond of methane occurs at the Fe single sites to produce Fe–CH_3, and this dissociated methyl was found to facilely transfer to the adjacent carbon site of SiC_2 by realizing the C–C coupling. Following this, hydrogen transfer occurs and ethylene is then produced *via* a key –CH-

Table 1 Comparison of the catalytic performance of the recently reported catalysts for the NOCM

Catalyst (metal loading)	Reaction conditions: Temperature, °C	Reaction conditions: Feed composition	Methane conversion, %	Selectivity for indicated products: C_6H_6	$C_{10}H_8$	Coke	Others	Ref.
Mo_6/MCM-22 (5 wt%)	700 °C	1500 mL g^{-1} h^{-1} CH_4/N_2 80/20	9% 5 h	66%	9%	16%	9%	24
Mo/ZSM-5	700 °C	1500 mL g^{-1} h^{-1} CH_4/N_2 80/20	11.6% 15 h	C_{6+}: 8.8%				26
10MoC_y/HZSM-5 (10 wt%)	700 °C	1550 mL g^{-1} h^{-1} CH_4/N_2 91/9	11.6% 15 h	80%	—	—	—	32
Mo/HZSM-5	700 °C	WHSV 2 h^{-1} CH_4/N_2 95/5	22.7% 16 h	51.5%	21.8%	C_7H_8: 3.2 C_8H_{10}: 17.3 C_2: 6.1		34
Mo_5/MCM-22 (21) (5 wt%)	680 °C	1500 mL g^{-1} h^{-1} CH_4/N_2 90/10	7.2% 2 h	51.9%	~7%	5.6%	34.4%	42
Mo_5/MCM-22 (91) (5 wt%)	680 °C	1500 mL g^{-1} h^{-1} CH_4/N_2 90/10	4.5% 2 h	36.1%	~7%	5%	51.1%	42
MoOx/ZSM-5 (3 wt%)	700 °C	1550 mL h^{-1} g^{-1} 9% N_2/CH_4	8% 12 h	62%	—	22%	16%	43
MoOx/ZSM-5 (10 wt%)	700 °C	1550 mL h^{-1} g^{-1} 9% N_2/CH_4	9.5% 12 h	85%	—	2%	13%	43
Mo/HZSM-5 (MA) (10 wt%)	700 °C	1500 mL g^{-1} h^{-1} CH_4/N_2 90/10	11.8% 10 h	70.7%	12.9%	9.3%	7.1%	44
Mo/H-S-Z (6 wt%)	700 °C	1500 mL g^{-1} h^{-1} CH_4/Ar 90.3/9.7	6.29% 3 h	55.6%	—	6.6%	37.8%	45
Mo/HZSM-5	700 °C	1500 mL g^{-1} h^{-1} CH_4/N_2 90/10	12% 10 h	83.3%	—	—	—	46
0.5% Re-4.0%Mo/ZSM-5	750 °C	1000 mL g^{-1} h^{-1} CH_4/99.99%	14.8% 20 min	54.05%	30.4%	13%	2%	47
0.5% Cr-5% Mo–SZ	700 °C	600 mL g^{-1} h^{-1} CH_4/N_2 90/10	13.5%	55%	—	11.49%	27.5%	48
1.0% Fe (nano)-5% Mo/HZSM-5	700 °C	1650 mL g^{-1} h^{-1} CH_4/Ar 10/1	14%	22%	3%	52.3%	22.7%	49
1.5% Fe (nano)-5% Mo/HZSM-5	700 °C	1650 mL g^{-1} h^{-1} CH_4/Ar 10/1	12%	17%	6%	57%	20%	49
Mg–Mo/HZSM-5	800 °C	1440 mL g^{-1} h^{-1} CH_4/Ar/CO_2 90/8/2	12.3% 1 h	68.4%	—	10.1%	—	50
6Mo-0.2Ni/ZSM-5	700 °C	1500 mL g^{-1} h^{-1} CH_4/N_2 91/9	9.8%, 10 h	35%	2.5%	59%	3.5%	51
6Mo-0.6Co/ZSM-5			5%, 10 h	30%	2.1%	57%	10.9%	
10 Mo -1K/HZSM-5	750 °C	—	28% 255 min	50%	—	47%	—	53
PtSn/SiO2–5%H_2	700 °C	5% CH_4 introduce to 25% H_2/He tank	0.05% 6 h	C_2H_4: 63% C_2H_6: 36%				55
Pt–Bi/ZSM-5	600–700 °C	—	2% 8 h	C_2H_4 + C_2H_6: >90%				56
GaN/SBA15	700 °C	567 h^{-1}	2.5% 8 h	C_2H_4: 97.4% C_3H_6: 2.04% C_6 + 0.6%				61
Fe/HMCM-22	750 °C	1500 mL g^{-1} h^{-1} CH_4/Ar 90/10	896 nmol/(gcat. s)	74.6%	15.1%	—	10.3%	73
Fe/HZSM-5	700 °C	3750 mL g^{-1} h^{-1} CH_4/He 50/50	1.3% 10 hours	22.5%	—	42%	35.5%	76
Fe©CRS (0.41 wt%)	1080 °C	8000 mL g^{-1} h^{-1} CH_4/H_2 50/50	6.9–5.8% 100 h	C2: 86.2%, C3–C5: ~6% Aromatics: ~8%, coke: ~1%				81
Fe©SiO_2 (0.5 wt%)	1030 °C	3200 mLg^{-1} h^{-1} CH_4/Ar 90/10	30%	C_2 and aromatic 99%				82
Fe©SiO_2 (0.5 wt%)	1090 °C	21.4 L g^{-1} h^{-1} CH_4/N_2 90/10	48.1%	28%	24%	C_2H_4: 48%		15
Pt_1@CeO_2 (0.5 wt%)	975 °C	6 L g^{-1} h^{-1} 1% CH_4/He	14.4%	~13%	~2%	C_2: 74.6% C_3: <10%		85

CH_2 intermediate on the Fe single-atom site and results in a carbon vacancy on the SiC_2 surface. Meanwhile, this carbon defect on the SiC_2 surface can be recovered by the activation of another methane on the Fe single-atom site. It thus involves the withdrawal and regeneration of the surface C atom on the support during methane conversion. The involvement of both C and Fe suggests the importance of the dual site synergetic interaction for the nonoxidative conversion of methane on the SACs. The dynamic formation mechanism of the $FeSiC_2$@SiO_2 from FeO_3©SiO_2 was further explored.[88] As shown in Fig. 12b,

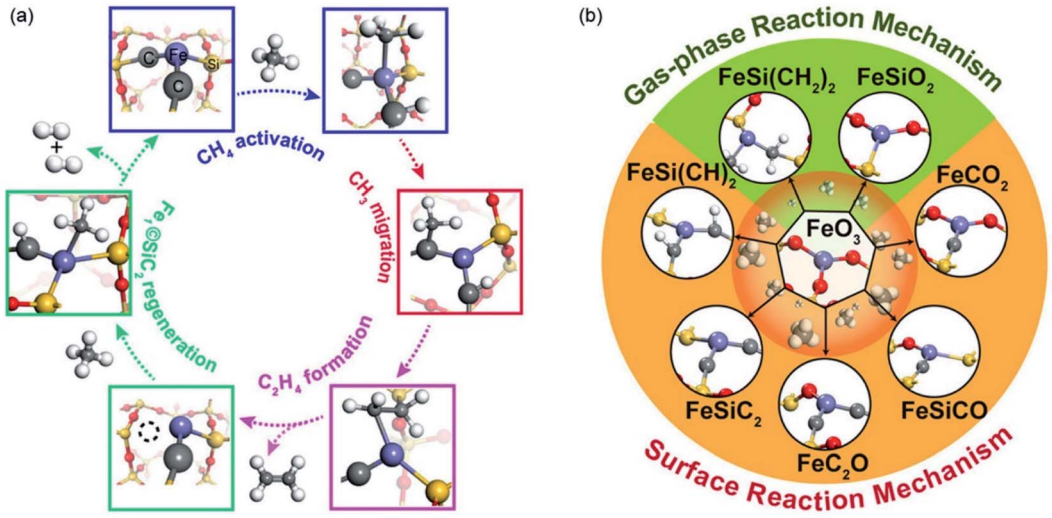

Fig. 12 (a) Proposed quasi Mars–van Krevelen mechanism for methane conversion over the Fe_1@SiC_2 active center. Reproduced with permission from ref. 87. Copyright 2020 John Wiley and Sons. (b) Theoretically revealed active centers evolving from FeO_3©SiO_2 during methane conversion. Reproduced with permission from ref. 88. Copyright 2020 American Chemical Society.

eight different active centers evolving from FeO_3©SiO_2 were monitored, which demonstrated different catalytic performances for methane conversion. The Fe active centers coordinated with unsaturated C atoms were revealed to be more active for methane dissociation, these prefer to transfer the dissociated methyl group to adjacent C atoms and follow a surface coupling reaction mechanism. Meanwhile, the Fe active centers coordinated with saturated C/O/Si were shown to have a reduced activity for methane conversion, which leads to the desorption of the methyl group into the gas phase and follows a gas-phase reaction mechanism. This highlights the importance of engineering active sites in determining the activity and selectivity in the NOCM, which should be considered in the design of further catalysts for methane conversion.

4. Summary and outlook

The direct conversion of methane to high-value chemicals is a highly economical way to utilize methane. In terms of the conventional zeolite supported Mo-based catalysts for the nonoxidative conversion of methane to aromatics, significant progress has been made, including identification of the active site, an explanation of the function of the zeolite, and the design of promoters. The nature of Mo species under real-time conditions, the pore structure with the acidity of the zeolite supports, as well as the synergy effect of promoters, play a crucial role in determining the catalytic activity and stability of methane nonoxidative coupling over Mo-based conventional catalysts. On the other hand, various non-Mo-based catalysts have been considered recently. In particular, SACs as a novel topic in heterogeneous catalysis have been demonstrated to possess significant potential in the nonoxidative conversion of methane. The single-atom active site of the SACs with the synergistic support enables an unusual catalytic behavior providing the olefins as a primary product in methane nonoxidative coupling, which makes it a newly emerging candidate in the area of methane chemistry.

Despite this, the activation of the C–H bond of methane and the selective controlling of C–C coupling is still a challenge in the nonoxidative conversion of methane. Further investigation of the structure–activity relationship in methane activation and coupling is greatly needed, not only for the conventional Mo-based catalysts but also in the development of novel catalysts. Recent experimental and theoretical results have demonstrated that the coordinatively unsaturated single-Fe-atom sites show significant potential for use in the NOCM. The activation of C–H bond occurs at the Fe single site and the adjacent carbon site is essential for C–C coupling. For example, elucidating the exact atomic structure of the active sites, especially in real-time reactions, with their associated electronic structure, acidic/basic properties and others, as well as the possible roles of neighboring chemical environments, would be important to correlate with the catalytic activity of the C–H bond activation. On the other hand, the catalysts also require functional sites for C–C coupling which determines the length of the carbon chain, and the dependency of the size and geometry of the active center seems to have a negligible effect on the product distributions. In this regard, the rational design of SACs with the desired coordination environment (such as C, Si, O coordination number) is considered as a promising route to achieving the efficient activation of the C–H bond and selective C–C coupling.

Furthermore, in-depth insights into the underlying mechanism of NOCM will require *in situ* characterization on the active phases and the experimental identification of the reaction intermediates under a high reaction temperature. To this end, techniques such as electron spin resonance (ESR) spectroscopy, Mössbauer spectroscopy, atomic resonance absorption spectroscopy, and so on can be employed. The development of spatially resolved reactors is also important for providing

insights into the gas-phase reaction intermediates. Theoretical modelling is a powerful tool to access information such as C–H bond breaking and C–C coupling, as well as determining the energy barriers during the whole process. In addition, the carburization and accumulation of carbonaceous species on the surface of the catalyst remain the main challenges under non-oxidative conditions. Therefore, the development of novel catalysts with a high activity, selectivity, and stability is still a long-pursued target.

We anticipate that further advances will be achieved in this field. Meanwhile, the direct carbon chain growth of methane with other carbon resources such as CO_2 is also a significant development in the area of methane conversion and application. Although the oxidative coupling of methane was studied extensively at the end of the last century, methane coupling using a modern catalytic technique is now welcoming in a new era in this field, and it also offers human beings a novel path for the rational utilization of natural resources.

Author contributions

Conceptualization, writing – original draft, writing – review & editing, T. Z.

Conflicts of interest

There are no conflicts to declare.

References

1 V. R. Choudhary, A. K. Kinage and T. V. Choudhary, Low-temperature nonoxidative activation of methane over H-galloaluminosilicate (MFI) zeolite, *Science*, 1997, **275**, 1286–1288.
2 S. H. Morejudo, R. Zanon, S. Escolastico, I. Yuste-Tirados, H. Malerod-Fjeld, P. K. Vestre, W. G. Coors, A. Martinez, T. Norby, J. M. Serra and C. Kjolseth, Direct conversion of methane to aromatics in a catalytic co-ionic membrane reactor, *Science*, 2016, **353**, 563–566.
3 P. Tang, Q. J. Zhu, Z. X. Wu and D. Ma, Methane activation: the past and future, *Energy Environ. Sci.*, 2014, **7**, 2580–2591.
4 J. J. Spivey and G. Hutchings, Catalytic aromatization of methane, *Chem. Soc. Rev.*, 2014, **43**, 792–803.
5 L. L. Sun, Y. Wang, N. J. Guan and L. D. Li, Methane Activation and Utilization: Current Status and Future Challenges, *Energy Technol.*, 2020, **8**, 1900826.
6 X. G. Meng, X. J. Cui, N. P. Rajan, L. Yu, D. H. Deng and X. H. Bao, Direct Methane Conversion under Mild Condition by Thermo-, Electro-, or Photocatalysis, *Chem*, 2019, **5**, 2296–2325.
7 P. Schwach, X. Pan and X. Bao, Direct Conversion of Methane to Value-Added Chemicals over Heterogeneous Catalysts: Challenges and Prospects, *Chem. Rev.*, 2017, **117**, 8497–8520.
8 S. Ma, X. Guo, L. Zhao, S. Scott and X. Bao, Recent progress in methane dehydroaromatization: From laboratory curiosities to promising technology, *J. Energy Chem.*, 2013, **22**, 1–20.
9 S. D. Senanayake, J. A. Rodriguez and J. F. Weaver, Low Temperature Activation of Methane on Metal-Oxides and Complex Interfaces: Insights from Surface Science, *Acc. Chem. Res.*, 2020, **53**, 1488–1497.
10 K. D. Sun, D. M. Ginosar, T. He, Y. L. Zhang, M. H. Fan and R. P. Chen, Progress in Nonoxidative Dehydroaromatization of Methane in the Last 6 Years, *Ind. Eng. Chem. Res.*, 2018, **57**, 1768–1789.
11 M. A. A. Aziz, A. A. Jalil, S. Wongsakulphasatch and D. V. N. Vo, Understanding the role of surface basic sites of catalysts in CO_2 activation in dry reforming of methane: a short review, *Catal. Sci. Technol.*, 2020, **10**, 35–45.
12 I. Vollmer, I. Yarulina, F. Kapteijn and J. Gascon, Progress in Developing a Structure-Activity Relationship for the Direct Aromatization of Methane, *Chemcatchem*, 2019, **11**, 39–52.
13 D. V. Golinskii, N. V. Vinichenko, E. V. Zatolokina, V. V. Pashkov, E. A. Paukshtis, T. I. Gulyaeva, P. E. Pavlyuchenko, O. V. Krol' and A. S. Belyi, Modern Catalysts and Methods of Nonoxidative Methane Conversion, *Russ. J. Gen. Chem.*, 2020, **90**, 1104–1119.
14 R. Horn and R. Schlögl, Methane Activation by Heterogeneous Catalysis, *Catal. Lett.*, 2015, **145**, 23–39.
15 X. Guo, G. Fang, G. Li, H. Ma, H. Fan, L. Yu, C. Ma, X. Wu, D. Deng, M. Wei, D. Tan, R. Si, S. Zhang, J. Li, L. Sun, Z. Tang, X. Pan and X. Bao, Direct, Nonoxidative Conversion of Methane to Ethylene, Aromatics, and Hydrogen, *Science*, 2014, **344**, 616–619.
16 L. Wang, L. Tao, M. Xie, G. Xu, J. Huang and Y. Xu, Dehydrogenation and aromatization of methane under non-oxidizing conditions, *Catal. Lett.*, 1993, **21**, 35–41.
17 P. L. Tan, The catalytic performance of Mo-impregnated HZSM-5 zeolite in CH_4 aromatization: Strong influence of Mo loading and pretreatment conditions, *Catal. Commun.*, 2018, **103**, 101–104.
18 R. W. Borry, Y. H. Kim, A. Huffsmith, J. A. Reimer and E. Iglesia, Structure and Density of Mo and Acid Sites in Mo-Exchanged H-ZSM5 Catalysts for Nonoxidative Methane Conversion, *J. Phys. Chem. B*, 1999, **103**, 5787–5796.
19 W. Li, G. D. Meitzner, R. W. Borry and E. Iglesia, Raman and X-Ray Absorption Studies of Mo Species in Mo/H-ZSM5 Catalysts for Non-Oxidative CH_4 Reactions, *J. Catal.*, 2000, **191**, 373–383.
20 W. Ding, S. Li, G. D Meitzner and E. Iglesia, Methane Conversion to Aromatics on Mo/H-ZSM5: Structure of Molybdenum Species in Working Catalysts, *J. Phys. Chem. B*, 2001, **105**, 506–513.
21 J.-P. Tessonnier, B. Louis, S. Rigolet, M. J. Ledoux and C. Pham-Huu, Methane dehydro-aromatization on Mo/ZSM-5: About the hidden role of Brønsted acid sites, *Appl. Catal., A*, 2008, **336**, 79–88.
22 J.-P. Tessonnier, B. Louis, S. Walspurger, J. Sommer, M.-J. Ledoux and C. Pham-Huu, Quantitative Measurement of the Brönsted Acid Sites in Solid Acids: Toward a Single-Site Design of Mo-Modified ZSM-5 Zeolite, *J. Phys. Chem. B*, 2006, **110**, 10390–10395.
23 N. Kosinov, F. J. A. G. Coumans, G. Li, E. Uslamin, B. Mezari, A. S. G. Wijpkema, E. A. Pidko and E. J. M. Hensen, Stable

Mo/HZSM-5 methane dehydroaromatization catalysts optimized for high-temperature calcination-regeneration, *J. Catal.*, 2017, **346**, 125–133.

24 I. Julian, J. L. Hueso, N. Lara, A. Sole-Daura, J. M. Poblet, S. G. Mitchell, R. Mallada and J. Santamaria, Polyoxometalates as alternative Mo precursors for methane dehydroaromatization on Mo/ZSM-5 and Mo/MCM-22 catalysts, *Catal. Sci. Technol.*, 2019, **9**, 5927–5942.

25 M. Agote-Aran, R. E. Fletcher, M. Briceno, A. B. Kroner, I. V. Sazanovich, B. Slater, M. E. Rivas, A. W. J. Smith, P. Collier, I. Lezcano-Gonzalez and A. M. Beale, Implications of the Molybdenum Coordination Environment in MFI Zeolites on Methane Dehydroaromatisation Performance, *Chemcatchem*, 2020, **12**, 294–304.

26 I. Julian, M. B. Roedern, J. L. Hueso, S. Irusta, A. K. Baden, R. Mallada, Z. Davis and J. Santamaria, Supercritical solvothermal synthesis under reducing conditions to increase stability and durability of Mo/ZSM-5 catalysts in methane dehydroaromatization, *Appl. Catal., B*, 2020, **263**, 118360.

27 D. Wang, J. H. Lunsford and M. P. Rosynek, Catalytic conversion of methane to benzene over Mo/ZSM-5, *Top. Catal.*, 1996, **3**, 289–297.

28 D. Wang, J. H. Lunsford and M. P. Rosynek, Characterization of a Mo/ZSM-5 Catalyst for the Conversion of Methane to Benzene, *J. Catal.*, 1997, **169**, 347–358.

29 H. Liu, X. Bao and Y. Xu, Methane dehydroaromatization under nonoxidative conditions over Mo/HZSM-5 catalysts: Identification and preparation of the Mo active species, *J. Catal.*, 2006, **239**, 441–450.

30 I. Lezcano-González, R. Oord, M. Rovezzi, P. Glatzel, S. W. Botchway, B. M. Weckhuysen and A. M. Beale, Molybdenum Speciation and its Impact on Catalytic Activity during Methane Dehydroaromatization in Zeolite ZSM-5 as Revealed by Operando X-Ray Methods, *Angew. Chem., Int. Ed.*, 2016, **55**, 5215–5219.

31 N. K. Razdan and A. Bhan, Carbidic Mo is the sole kinetically-relevant active site for catalytic methane dehydroaromatization on Mo/H-ZSM-5, *J. Catal.*, 2020, **389**, 667–676.

32 M. Rahman, A. Sridhar and S. J. Khatib, Impact of the presence of Mo carbide species prepared ex situ in Mo/HZSM-5 on the catalytic properties in methane aromatization, *Appl. Catal., A*, 2018, **558**, 67–80.

33 Z. R. Ismagilov, E. V. Matus and L. T. Tsikoza, Direct conversion of methane on Mo/ZSM-5 catalysts to produce benzene and hydrogen: achievements and perspectives, *Energy Environ. Sci.*, 2008, **1**, 526–541.

34 N. Kosinov, F. J. A. G. Coumans, E. A. Uslamin, A. S. G. Wijpkema, B. Mezari and E. J. M. Hensen, Methane Dehydroaromatization by Mo/HZSM-5: Mono- or Bifunctional Catalysis?, *ACS Catal.*, 2017, **7**, 520–529.

35 H. F. Li, L. X. Jiang, Y. X. Zhao, Q. Y. Liu, T. Zhang and S. G. He, Formation of Acetylene in the Reaction of Methane with Iron Carbide Cluster Anions FeC_3- under High-Temperature Conditions, *Angew. Chem., Int. Ed.*, 2018, **57**, 2662–2666.

36 T. Zhang, X. Yang and Q. Ge, A DFT study of methane conversion on Mo-terminated Mo_2C carbides: Carburization *vs*. CC coupling, *Catal. Today*, 2020, **368**, 140–147.

37 T. Zhang, X. Yang and Q. Ge, CH_4 Dissociation and C-C Coupling on Mo-terminated MoC Surfaces: A DFT Study, *Catal. Today*, 2020, **339**, 54–61.

38 C.-L. Zhang, S. Li, Y. Yuan, W.-X. Zhang, T.-H. Wu and L.-W. Lin, Aromatization of methane in the absence of oxygen over Mo-based catalysts supported on different types of zeolites, *Catal. Lett.*, 1998, **56**, 207–213.

39 H. Zheng, D. Ma, X. Bao, J. Z. Hu, J. H. Kwak, Y. Wang and C. H. F. Peden, Direct Observation of the Active Center for Methane Dehydroaromatization Using an Ultrahigh Field ^{95}Mo NMR Spectroscopy, *J. Am. Chem. Soc.*, 2008, **130**, 3722–3723.

40 J. Z. Hu, J. H. Kwak, Y. Wang, C. H. F. Peden, H. Zheng, D. Ma and X. Bao, Studies of the Active Sites for Methane Dehydroaromatization Using Ultrahigh-Field Solid-State ^{95}Mo NMR Spectroscopy, *J. Phys. Chem. C*, 2009, **113**, 2936–2942.

41 D. Ma, Y. Lu, L. Su, Z. Xu, Z. Tian, Y. Xu, L. Lin and X. Bao, Remarkable Improvement on the Methane Aromatization Reaction: A Highly Selective and Coking-Resistant Catalyst, *J. Phys. Chem. B*, 2002, **106**, 8524–8530.

42 T. H. Lim, K. Nam, I. K. Song, K. Y. Lee and D. H. Kim, Effect of Si/Al_2 ratios in Mo/H-MCM-22 on methane dehydroaromatization, *Appl. Catal., A*, 2018, **552**, 11–20.

43 M. Rahman, A. Infantes-Molina, A. S. Hoffman, S. R. Bare, K. L. Emerson and S. J. Khatib, Effect of Si/Al ratio of ZSM-5 support on structure and activity of Mo species in methane dehydroaromatization, *Fuel*, 2020, **278**, 118290.

44 P. L. Tan, Ammonia-basified 10 wt% Mo/HZSM-5 material with enhanced dispersion of Mo and performance for catalytic aromatization of methane, *Appl. Catal., A*, 2019, **580**, 111–120.

45 P. Zhu, G. Yang, J. Sun, R. Fan, P. Zhang, Y. Yoneyama and N. Tsubaki, A hollow Mo/HZSM-5 zeolite capsule catalyst: preparation and enhanced catalytic properties in methane dehydroaromatization, *J. Mater. Chem. A*, 2017, **5**, 8599–8607.

46 X. Huang, X. Jiao, M. G. Lin, K. Wang, L. T. Jia, B. Hou and D. B. Lia, Coke distribution determines the lifespan of a hollow Mo/HZSM-5 capsule catalyst in CH_4 dehydroaromatization, *Catal. Sci. Technol.*, 2018, **8**, 5753–5762.

47 A. A. Stepanov, V. I. Zaikovskii, L. L. Korobitsyna and A. V. Vosmerikov, Nonoxidative Conversion of Methane to Aromatic Hydrocarbons in the Presence of ZSM-5 Zeolites Modified with Molybdenum and Rhenium, *Pet. Chem.*, 2019, **59**, 91–98.

48 M. A. Abedin, S. Kanitkar, S. Bhattar and J. J. Spivey, Promotional Effect of Cr in Sulfated Zirconia-Based Mo Catalyst for Methane Dehydroaromatization, *Energy Technol.*, 2020, **8**, 1900555.

49 K. D. Sun, W. B. Gong, K. Gasem, H. Adidharma, M. H. Fan and R. P. Chen, Catalytic Methane Dehydroaromatization with Stable Nano Fe Doped on Mo/HZSM-5 Synthesized with a Simple and Environmentally Friendly Method and Clarification of a Perplexing Catalysis Mechanism Dilemma in This Field for a Period of Time, *Ind. Eng. Chem. Res.*, 2017, **56**, 11398–11412.

50 X. Cheng, P. Yan, X. Z. Zhang, F. Yang, C. Y. Dai, D. P. Li and X. X. Ma, Enhanced methane dehydroaromatization in the presence of CO_2 over Fe- and Mg-modified Mo/ZSM-5, *Mol. Catal.*, 2017, **437**, 114–120.

51 A. Sridhar, M. Rahman, A. Infantes-Molina, B. J. Wylie, C. G. Borcik and S. J. Khatib, Bimetallic Mo-Co/ZSM-5 and Mo-Ni/ZSM-5 catalysts for methane dehydroaromatization: A study of the effect of pretreatment and metal loadings on the catalytic behavior, *Appl. Catal., A*, 2020, **589**, 117247.

52 D. Bajec, A. Kostyniuk, A. Pohar and B. Likozar, Nonoxidative methane activation, coupling, and conversion to ethane, ethylene, and hydrogen over Fe/HZSM-5, Mo/HZSM-5, and Fe-Mo/HZSM-5 catalysts in packed bed reactor, *Int. J. Energy Res.*, 2019, **43**, 6852–6868.

53 V. Ramasubramanian, D. J. Lienhard, H. Ramsurn and G. L. Price, Effect of Addition of K, Rh and Fe Over Mo/HZSM-5 on Methane Dehydroaromatization Under Non-oxidative Conditions, *Catal. Lett.*, 2019, **149**, 950–964.

54 M. Belgued, P. Pareja, A. Amariglio and H. Amariglio, Conversion of methane into higher hydrocarbons on platinum, *Nature*, 1991, **352**, 789–790.

55 D. Gerceker, A. H. Motagamwala, K. R. Rivera-Dones, J. B. Miller, G. W. Huber, M. Mavrikakis and J. A. Dumesic, Methane Conversion to Ethylene and Aromatics on PtSn Catalysts, *ACS Catal.*, 2017, **7**, 2088–2100.

56 Y. Xiao and A. Varma, Highly Selective Nonoxidative Coupling of Methane over Pt-Bi Bimetallic Catalysts, *ACS Catal.*, 2018, **8**, 2735–2740.

57 D. Soulivong, S. Norsic, M. Taoufik, C. Coperet, J. Thivolle-Cazat, S. Chakka and J.-M. Basset, Non-Oxidative Coupling Reaction of Methane to Ethane and Hydrogen Catalyzed by the Silica-Supported Tantalum Hydride: $(\equiv SiO)_2Ta-H$, *J. Am. Chem. Soc.*, 2008, **130**, 5044–5045.

58 N. Levin, J. Lengyel, J. F. Eckhard, M. Tschurl and U. Heiz, Catalytic Non-Oxidative Coupling of Methane on $Ta_8O_2^+$, *J. Am. Chem. Soc.*, 2020, **142**, 5862–5869.

59 M. V. Luzgin, A. A. Gabrienko, V. A. Rogov, A. V. Toktarev, V. N. Parmon and A. G. Stepanov, The "Alkyl" and "Carbenium" Pathways of Methane Activation on Ga-Modified Zeolite BEA: 13C Solid-State NMR and GC-MS Study of Methane Aromatization in the Presence of Higher Alkane, *J. Phys. Chem. C*, 2010, **114**, 21555–21561.

60 K. Dutta, V. Chaudhari, C. J. Li and J. Kopyscinski, Methane conversion to ethylene over GaN catalysts. Effect of catalyst nitridation, *Appl. Catal., A*, 2020, **595**, 117430.

61 K. Dutta, M. Shahryari and J. Kopyscinski, Direct Nonoxidative Methane Coupling to Ethylene over Gallium Nitride: A Catalyst Regeneration Study, *Ind. Eng. Chem. Res.*, 2020, **59**, 4245–4256.

62 V. R. Choudhary, K. C. Mondal and S. A. Mulla, Simultaneous conversion of methane and methanol into gasoline over bifunctional Ga-, Zn-, In-, and/or Mo-modified ZSM-5 zeolites, *Angew. Chem., Int. Ed.*, 2005, **44**, 4381–4385.

63 T. Gong, L. Qin, J. Lu and H. Feng, ZnO modified ZSM-5 and Y zeolites fabricated by atomic layer deposition for propane conversion, *Phys. Chem. Chem. Phys.*, 2016, **18**, 601–614.

64 M. V. Luzgin, V. A. Rogov, S. S. Arzumanov, A. V. Toktarev, A. G. Stepanov and V. N. Parmon, Understanding Methane Aromatization on a Zn-Modified High-Silica Zeolite, *Angew. Chem., Int. Ed.*, 2008, **47**, 4559–4562.

65 J. F. Wu, W. D. Wang, J. Xu, F. Deng and W. Wang, Reactivity of C1 Surface Species Formed in Methane Activation on Zn-Modified H-ZSM-5 Zeolite, *Chem.–Eur. J.*, 2010, **16**, 14016–14025.

66 A. A. Gabrienko, S. S. Arzumanov, A. V. Toktarev, I. G. Danilova, I. P. Prosvirin, V. V. Kriventsov, V. I. Zaikovskii, D. Freude and A. G. Stepanov, Different Efficiency of Zn_2^+ and ZnO Species for Methane Activation on Zn-Modified Zeolite, *ACS Catal.*, 2017, **7**, 1818–1830.

67 A. A. Gabrienko, S. S. Arzumanov, M. V. Luzgin, A. G. Stepanov and V. N. Parmon, Methane Activation on Zn_2^+-Exchanged ZSM-5 Zeolites. The Effect of Molecular Oxygen Addition, *J. Phys. Chem. C*, 2015, **119**, 24910–24918.

68 G. Qi, Q. Wang, J. Xu, J. Trébosc, O. Lafon, C. Wang, J.-P. Amoureux and F. Deng, Synergic Effect of Active Sites in Zinc-Modified ZSM-5 Zeolites as Revealed by High-Field Solid-State NMR Spectroscopy, *Angew. Chem., Int. Ed.*, 2016, **55**, 15826–15830.

69 P. He, A. G. Wang, S. J. Meng, G. M. Bernard, L. J. Liu, V. K. Michaelis and H. Song, Impact of Al sites on the methane co-aromatization with alkanes over Zn/HZSM-5, Catal, *Today*, 2019, **323**, 94–104.

70 B. M. Weckhuysen, D. Wang, M. P. Rosynek and J. H. Lunsford, Conversion of Methane to Benzene over Transition Metal Ion ZSM-5 Zeolites: I. Catalytic Characterization, *J. Catal.*, 1998, **175**, 338–346.

71 B. M. Weckhuysen, D. Wang, M. P. Rosynek and J. H. Lunsford, Conversion of Methane to Benzene over Transition Metal Ion ZSM-5 Zeolites: II. Catalyst Characterization by X-Ray Photoelectron Spectroscopy, *J. Catal.*, 1998, **175**, 347–351.

72 S. Takenaka, M. Serizawa and K. Otsuka, Formation of filamentous carbons over supported Fe catalysts through methane decomposition, *J. Catal.*, 2004, **222**, 520–531.

73 P. L. Tan, Active phase, catalytic activity, and induction period of Fe/zeolite material in nonoxidative aromatization of methane, *J. Catal.*, 2016, **338**, 21–29.

74 J. P. Sim, B. J. Lee, G. H. Han, D. H. Kim and K. Y. Lee, Promotional effect of Au on Fe/HZSM-5 catalyst for methane dehydroaromatization, *Fuel*, 2020, **274**, 117852.

75 B. Qiao, A. Wang, X. Yang, L. F. Allard, Z. Jiang, Y. Cui, J. Liu, J. Li and T. Zhang, Single-atom catalysis of CO oxidation using Pt_1/FeO_x, *Nat. Chem.*, 2011, **3**, 634–641.

76 Y. Lai and G. Veser, The nature of the selective species in Fe-HZSM-5 for non-oxidative methane dehydroaromatization, *Catal. Sci. Technol.*, 2016, **6**, 5440–5452.
77 B. R. Wood, J. A. Reimer, A. T. Bell, M. T. Janicke and K. C. Ott, Methanol formation on Fe/Al-MFI via the oxidation of methane by nitrous oxide, *J. Catal.*, 2004, **225**, 300–306.
78 H. Schwarz, Chemistry with Methane: Concepts Rather than Recipes, *Angew. Chem., Int. Ed.*, 2011, **50**, 10096–10115.
79 E. W. McFarland and H. Metiu, Catalysis by Doped Oxides, *Chem. Rev.*, 2013, **113**, 4391–4427.
80 P. Sot, M. A. Newton, D. Baabe, M. D. Walter, A. P. van Bavel, A. D. Horton, C. Coperet and J. A. van Bokhoven, Non-oxidative Methane Coupling over Silica versus Silica-Supported Iron(II) Single Sites, *Chem.–Eur. J.*, 2020, **26**, 8012–8016.
81 S. J. Han, S. W. Lee, H. W. Kim, S. K. Kim and Y. T. Kim, Nonoxidative Direct Conversion of Methane on Silica-Based Iron Catalysts: Effect of Catalytic Surface, *ACS Catal.*, 2019, **9**, 7984–7997.
82 M. Sakbodin, Y. Q. Wu, S. C. Oh, E. D. Wachsman and D. X. Liu, Hydrogen-Permeable Tubular Membrane Reactor: Promoting Conversion and Product Selectivity for Non-Oxidative Activation of Methane over an Fe (c) SiO_2 Catalyst, *Angew. Chem., Int. Ed.*, 2016, **55**, 16149–16152.
83 A. T. Bell, Single iron sites for catalytic, nonoxidative conversion of methane, *Sci. China: Chem.*, 2014, **57**, 923.
84 D. Bajec, A. Kostyniuk, A. Pohar and B. Likozar, Micro-kinetics of non-oxidative methane coupling to ethylene over Pt/CeO_2 catalyst, *Chem. Eng. J.*, 2020, **396**, 125182.
85 P. F. Xie, T. C. Pu, A. M. Nie, S. Hwang, S. C. Purdy, W. J. Yu, D. Su, J. T. Miller and C. Wang, Nanoceria-Supported Single-Atom Platinum Catalysts for Direct Methane Conversion, *ACS Catal.*, 2018, **8**, 4044–4048.
86 Z. Q. Huang, T. Y. Zhang, C. R. Chang and J. Li, Dynamic Frustrated Lewis Pairs on Ceria for Direct Nonoxidative Coupling of Methane, *ACS Catal.*, 2019, **9**, 5523–5536.
87 Y. Liu, J.-C. Liu, T.-H. Li, Z.-H. Duan, T.-Y. Zhang, M. Yan, W.-L. Li, H. Xiao, Y.-G. Wang, C.-R. Chang and J. Li, Unravelling the Enigma of Nonoxidative Conversion of Methane on Iron Single-Atom Catalysts, *Angew. Chem., Int. Ed.*, 2020, **132**, 18745–18749.
88 T. H. Li, M. Yan, Y. Liu, Z. Q. Huang, C. R. Chang and J. Li, Cooperative Catalysis by Multiple Active Centers in Nonoxidative Conversion of Methane, *J. Phys. Chem. C*, 2020, **124**, 13656–13663.
89 T. Z. H. Gani and H. J. Kulik, Understanding and Breaking Scaling Relations in Single-Site Catalysis: Methane to Methanol Conversion by Fe-IV=O, *ACS Catal.*, 2018, **8**, 975–986.
90 X. F. Ma, K. J. Sun, J. X. Liu, W. X. Li, X. M. Cai and H. Y. Su, Single Ru Sites-Embedded Rutile TiO_2 Catalyst for Non-Oxidative Direct Conversion of Methane: A First-Principles Study, *J. Phys. Chem. C*, 2019, **123**, 14391–14397.